IET Nanobiotechnology

Research Article

IET Journals
The Institution of Engineering and Technology

Enhanced wound healing activity of Ag–ZnO composite NPs in Wistar Albino rats

ISSN 1751-8741
Received on 5th April 2017
Revised 9th December 2017
Accepted on 15th December 2017
E-First on 14th March 2018
doi: 10.1049/iet-nbt.2017.0087
www.ietdl.org

Sravani Kantipudi[1], Jhansi Rani Sunkara[1], Muralikrishna Rallabhandi[1], Chandi Vishala Thonangi[2], Raga Deepthi Cholla[2], Pratap Kollu[3,4], Madhu Kiran Parvathaneni[5], Sri Venkata Narayana Pammi[6] ✉

[1]School of Chemistry, Andhra University, Visakhapatnam 533 003, India
[2]Pharmacy Department, Andhra University, Visakhapatnam 533 003, India
[3]School of Physics, University of Hyderabad, Gachibowli, Hyderabad 500 046, India
[4]Thin Film Magnetism Group, Cavendish Laboratory, Department of Physics, University of Cambridge, Cambridge CB3 0HE, UK
[5]Department of Biotechnology, University of Science and Technology, Harrisburg, PA 17101, USA
[6]Department of Materials Science and Engineering, Chungnam National University, Daeduk Science Town, 305-764 Daejeon, Korea
✉ *E-mail: sreepammi@gmail.com*

Abstract: In the present study, silver (Ag) and Ag–zinc oxide (ZnO) composite nanoparticles (NPs) were synthesised and studied their wound-healing efficacy on rat model. Ultraviolet–visible spectroscopy of AgNPs displayed an intense surface plasmon (SP) resonance absorption at 450 nm. After the addition of aqueous Zn acetate solution, SP resonance band has shown at 413.2 nm indicating a distinct blue shift of about 37 nm. X-ray diffraction analysis Ag–ZnO composite NPs displayed existence of two mixed sets of diffraction peaks, i.e. both Ag and ZnO, whereas AgNPs exhibited face-centred cubic structures of metallic Ag. Scanning electron microscope (EM) and transmission EM analyses of Ag–ZnO composite NPs revealed the morphology to be monodispersed hexagonal and quasi-hexagonal NPs with distribution of particle size of 20–40 nm. Furthermore, the authors investigated the wound-healing properties of Ag–ZnO composite NPs in an animal model and found that rapid healing within 10 days when compared with pure AgNPs and standard drug dermazin.

1 Introduction

Nanotechnology, due to its capability of modulating metals into their nanosize drastically changes the chemical, physical and optical properties of metals; hence, it is gaining tremendous impetus in the present century. Skin acts as a protective barrier against environment for various living organisms including mankind. Loss of even small portions of the skin may lead to a chronic state and major disability when left untreated. Hence, wound which resulted due to loss of integrity of the skin must be treated so as to achieve wound healing by conversion of the wound into an aesthetically satisfactory scar. In present days, vast research activities have been carried out in order to discover better healing agents as this has been one of the promising tasks in the current generation [1]. Various studies have been carried out using different models in order to evaluate the wound-healing phenomenon [2–4].

Silver nanoparticles (AgNPs) can be considered for wound-healing evaluation process as it has wide applications in medicinal domains. The bactericidal activity of AgNPs against drug-sensitive and multi-drug-resistant (MDR) pathogenic bacteria has been studied by our group (human and fish bacterial pathogens) and many scientists and it was proved to be a powerful weapon against MDR and wound-healing applications [1, 5–13]. However, there is significant evidence related to cytotoxicity and genotoxicity of AgNPs to human normal cells [13, 14]. To control the cytotoxicity of AgNPs, the loading of the metal oxides on AgNPs is an effective way to reduce the amount of Ag ion release in the mean time without jeopardising its functionality [15, 16]. In addition, nano-zinc oxide (ZnO) has been reported for wound-healing applications as one of the highly stable and non-toxic inorganic antibacterial material [17]. However, the limited antibacterial activity of ZnO makes these composite dressings less effective in treating wounds infected with MDR. In addition, these Ag–ZnO composites may inhibit the growth of bacteria synergistically due to the strong interaction between Ag and ZnO. In addition to the activity of AgNPs, Zn also plays a critical role in skin functioning as it enhances collagen synthesis which would assist the process of wound healing. Moreover, Zn has its own importance in the epithelialisation of skin [18].

Hence in the present work, we focused on the preparation and characterisation of Ag and Ag–ZnO composite NPs by wet chemical method using teflon-coated autoclave. Furthermore, we expected Ag–ZnO composite NPs might be a potential candidate for wound healing for biomedical application, because it has enhanced antibacterial activity and low cytotoxicity by tuning the release of Ag ions slowly by making composite with ZnO. To examine wound-healing efficacy on rat model, Ag and Ag–ZnO composite NPs were formulated into a gel using the gel base Carbapol 934. Apart from gelling agents, i.e. alginic acid, bentonite etc., we chose carbapol as gel base, because of its unique properties such as effectiveness in its formulations such as emulsions, suspensions, transdermals, sustained release formulations, topicals etc. It also helps in formation of clear gels when treated with water. Carbapol gel prepared is highly stable and is having good rheological properties. Ag and Ag–ZnO composite NPs formulated as gel were evaluated for wound-healing activity on Albino Wistar rats via visual observation, histology study of skin.

2 Experimental section

2.1 Methods

Oleic acid (OAc, 90%), oleyl amine (OAm, 80%), 1-dodecanol, Ag acetate [Ag (ac), 99.5%] and Zn (ac) were purchased from Sigma-Aldrich. All these reagents were used without any further purification for preparation of Ag and Ag–ZnO composite NPs. Carbapol, used for drug formulation is procured from the local pharmaceutical markets, stored at room temperature. Ketamine, used as anaesthesia for animals was procured as a gift sample from the Department of Pharmacy, Andhra University, Visakhapatnam.

© The Institution of Engineering and Technology 2017

2.2 Experimental animals

The male Albino Wistar rats weighing 180–200 g were used for *in vivo* studies and obtained from animal laboratory, Mahaveer enterprises, Hyderabad. The experiments were conducted in accordance with the principles given for the laboratory animal use and internationally accepted experimental protocols were provided by the Institutional Animal Ethical Committee. The rats were housed in cages made of polypropylene in a healthy atmosphere; they were regularly fed with standard rodent diet, water and libitum.

2.3 Drugs

Dermazin, antibacterial drug was used as the local chemotherapeutic agent for treatment and prevention of wounds, burns etc. was purchased from local pharmaceutical markets. The dermazin cream contains 1% micronised Ag sulphadiazine in a hydrophilic gel.

2.4 Preparation of AgNPs and Ag–ZnO composite NPs

OAc (0.5 ml), OAm (0.5 ml) and 1-dodecanol (5 ml) were added in a clean 50 ml beaker; the mixture is heated to 220°C under constant magnetic stirring. On reaching the required temperature, Ag (ac) is added in the reaction beaker and is placed in an autoclave, continued for 1 h at 220°C. The resulting dark brown solution was cooled down to room temperature, and is divided into two equal halves. One half of the product was precipitated by adding ethanol and the resulting solution is centrifuged using Remi-R8C centrifuge at 1000 rpm for 5–10 min, further purified by washing with hexane and ethanol alternatively. Another half dark brown solution obtained is added with Zn (ac) in ratio of 1:3 and reaction mixture is heated in an autoclave at 160°C for 2 h. The resulting solution was cooled down to room temperature and the product is collected after centrifugation, repeated washings with ethanol. The final product obtained is stored for evaluation.

2.5 Characterisation of AgNPs and Ag–ZnO composite NPs

The optical properties of AgNPs and Ag–ZnO composite NPs were analysed using ultraviolet–visible (UV–vis) spectra analysis (UV 1800, SHIMADZU). The structural and surface morphology of synthesised NPs were studied using X-ray diffraction (XRD) and scanning electron microscope (SEM) of composite NP's was studied using XRD [D8-Focus, Brucker instrument, Germany with copper ka radiation ($\lambda = 1.5406$ A°)] SEM (JSM-6610LV). Transmission EM (TEM) analysis is done by using a TEM, JEM-1200EX, JEOL Ltd., Japan.

2.6 Formulation of AgNPs and Ag–ZnO composite NPs gel

AgNPs and Ag–ZnO composite NPs prepared by the above said process were formulated into gel using the Carbapol 934 as gel base. Carbapol (also known as carbomer) is used for gel base as it is effective even in concentration of 0.5–2%. Initially carbapol was taken, lumps were destroyed if any, added with distiled water to make gel of 2% concentration. Bath sonicator is used for degasing, continuous stirring results in formation of gel with required consistency, if required a small amount of triethanol amine is added to get the required viscosity. Furthermore, two portions of gel were mixed with required concentrations of AgNPs and Ag–ZnO composite NPs individually using pestle and mortar which are used for *in vivo* studies. However, in the present paper we have used 0.1 g NP was used for preparation of gel to examine the wound-healing activity.

2.7 Evaluation of wound-healing activity by in vivo studies

Excision wound model is selected in order to evaluate the wound-healing activity in adult male Albino Wistar rats. Adult rats weighing about 180–200 g were selected and were grown in hygienic environmental conditions to make them pathogen free for the evaluation process. The animals were made sedentary by using anaesthesia, ketamine (80 mg/kg of rat). The dorsal fur of the animals was shaved with an electric clipper and the proposed area, where the wound is to be created was outlined on the dorsal side of the animals. An excision wound of 4 cm length and 2 mm depth was made for all the animals. These animals were made into four groups. After achieving haemostasis, the wound is left untreated in group 1, treated with dermazin (standard drug) in group 2, treated with AgNP's in group 3, treated with Ag–ZnO nanocomposite in group 4. Each group has three animals. The consequent change in the wound area was monitored day by day and the various parameters were determined at regular intervals.

2.8 Percentage of wound contraction

Wound healing is a process in which damaged skin is treated, so that the wound is restored into its normal state and the wound contraction is a process in which the wound undergoes shrinkage. Wound area was measured to find out the closure in wound area at different periods of treatment. The progressive changes in the area of the wound created, percentage reduction in the original wound size was expressed in terms of wound contraction (see equation below)

$$\text{wound contraction}\% = 1 - (A_d/A_0) \times 100$$

(A_0 = wound area on day zero, A_d = wound care on corresponding days)

2.9 Histopathological studies

Understanding the various changes during the process of treatment is important in assessing the efficiency of wound-healing process. The skin tissue samples were collected at 5th and 10th days at the site of the wound in different groups for evaluation of the extent of wound healing by histopathological studies. Biopsy specimens were collected with utmost care, preserved using 10% buffered formalin and are given for pathology studies, where they are stained using haemotoxylin and eosin.

2.10 Photographs

The photographs of wound from different groups were taken at specific intervals for visual comparison, and histology photographs are also presented to assist the results.

2.11 Statistical analysis

The results were expressed as mean ± standard deviation (SD). To establish statistical significance, the values were analysed using analysis of variance method. The analysis was carried out using GraphPad Prism software (version 4.0).

3 Results and discussion

3.1 Characterisation of NPs

The appearance of dark brown colour in the reaction mixture clearly indicates the formation of AgNP's during the reaction. Later, the appearance of light brown colour on the addition of Zn (ac) indicates the formation of composite. The brown colour of the solution in the reaction mixture is mainly due to the excitation of surface plasmon (SP) vibrations in the AgNPs. Fig. 1 shows the UV–vis absorption spectroscopy for AgNP's and Ag–ZnO nanocomposite. AgNPs and Ag–ZnO composite NPs displayed an intense SP resonance (SPR) absorption at 450 nm. After the addition of aqueous Zn (ac) solution for synthesis of Ag–ZnO composite NPs, SPR band has shown at 413.2 nm indicating a distinct blue shift of about 37 nm. This could be attributed to the

© The Institution of Engineering and Technology 2017

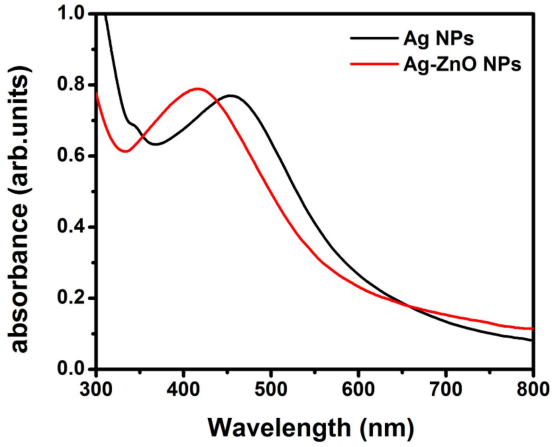

Fig. 1 *UV–vis spectra of as-synthesised Ag and Ag–ZnO NPs*

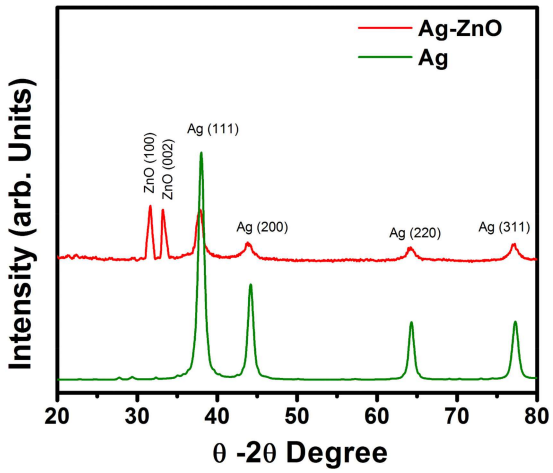

Fig. 2 *XRD pattern of as-prepared Ag and Ag–ZnO NPs*

formation of the oxide on the surface of AgNPs in order to form composite NPs. It has been previously demonstrated that the SPR band is highly sensitive to a variety of perturbations on the particle surface. The blue shift in SPR band position is expected for Ag colloidal particles as they become encapsulated with ZnO [19]. Furthermore, we have examined the crystal structure of pure AgNPs and Ag–ZnO composite NPs via XRD. From the obtained XRD pattern (Fig. 2) of synthesised Ag and Ag–ZnO composite NPs shows crystalline nature. XRD 2θ values of AgNPs, 38.25°, 44.48°, 64.59° and 77.52° correspond to (111), (200), (220) and (311) sets of lattice planes, respectively, that might be indexed as face-centred cubic structures of metallic Ag (JCPDS No. 04–0783). On the other hand, Ag–ZnO composite NPs displayed existence of two mixed sets of diffraction peaks (both Ag and ZnO). The 2θ values of Ag–ZnO composite NPs displayed at 31.82 and 34.54° represent the lattice planes (100) and (002) of hexagonal wurtzite structure of ZnO and 38.25°, 44.48°, 64.59° and 77.52° corresponding to (111), (200), (220) and (311) of face-centred cubic structures of metallic Ag, respectively. In addition, there is evidence that there are no large shifts in the positions of the diffraction peaks, which further confirm that the as-synthesised NPs are composed of ZnO and Ag phases indicating formation of Ag–ZnO composite NPs. It is interesting to note that, in case of Ag–ZnO composite NPs, relatively low intensity peaks of ZnO indicates low crystallinity of ZnO compared with Ag. The absence of other impurity peaks indicates high purity of Ag and Ag–ZnO composite NPs (Fig 3).

Furthermore, examination of surface morphology and exact particle size of Ag and Ag–ZnO composite NPs were analysed by SEM and TEM analyses (Figs. 4*a–f*). SEM image of AgNPs shows the presence of some large particles which might be attributed from evaporation of solvent during drying and/or agglomeration of small-sized particles (Fig. 4*a*). Surprisingly, Ag–ZnO composite NPs are clearly dispersed with hexagonal/quasi-hexagonal in shape

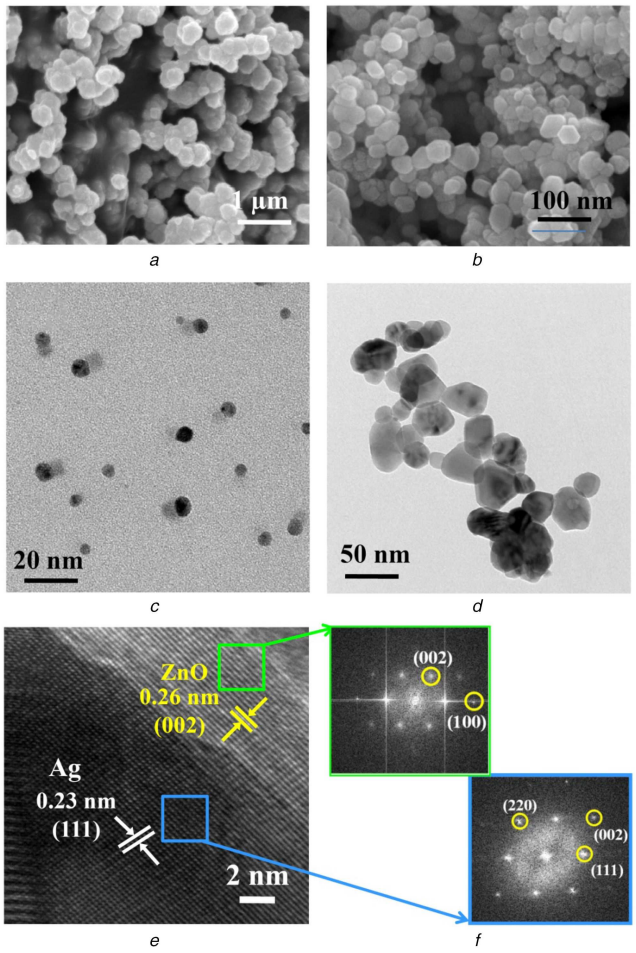

Fig. 3 *SEM and TEM images*

(a), (b) SEM images, ***(c), (d)*** TEM images of as-prepared Ag and Ag–ZnO NPs, respectively, ***(e)*** HRTEM image of Ag–ZnO composite NPs, ***(f)*** Selected-area FFT pattern of selected areas indicated by blue (Ag) and green (ZnO) squares

with particle size distribution between 25 and 40 nm (Fig. 4*b*). Further TEM image of AgNPs displayed spherical shaped particles with sizes from 8 to 12 nm in a well-dispersed state (Fig. 4*c*), whereas TEM image of Ag–ZnO composite NPs exhibited various morphologies with particle size distribution between 20 and 40 nm. It can be noted that some particles show hexagonal/quasi-hexagonal in shape as shown in Fig. 4*d*. Figs. 4*e* and *f* show a high-resolution TEM (HRTEM) image and a selected-area fast Fourier transform (FFT) pattern, respectively. From HRTEM image, there are two lattice spacing between adjacent lattice planes of 0.23 and 0.26 nm, and are clearly displayed from two regions. The lattice spacing of 0.23 nm indicates metallic Ag with face-centred cubic structure with preferential orientation (111) and 0.26 represents ZnO of preferred orientation (002) with hexagonal wurtzite structure. The FFT pattern has been taken from two regions indicated by selected area. The spots in FFT pattern can be indexed as (111), (200), (220) from metallic Ag and (100) and (002) from ZnO regions, respectively. These results were confirmed from the formation of Ag–ZnO composite NPs (Fig 5).

3.2 Wound-healing treatment in vivo studies

Ag–ZnO composite NPs showed a prominent role in the process of wound healing in the earlier stages itself. During the second day of drug application, the percentage healing in Ag–ZnO-treated animals was found to be significantly better than others. In case of native standard drug used for the recovery of animals, it was found to be very slow. In case of formulation of the gel containing Ag–ZnO composite NPs, the concentration of the drug was found to be nearly 0.1%. This is mainly based on the assumption that NPs usually have better pharmacokinetic properties, and hence more therapeutic action that could be achieved even in the low dosage

© The Institution of Engineering and Technology 2017

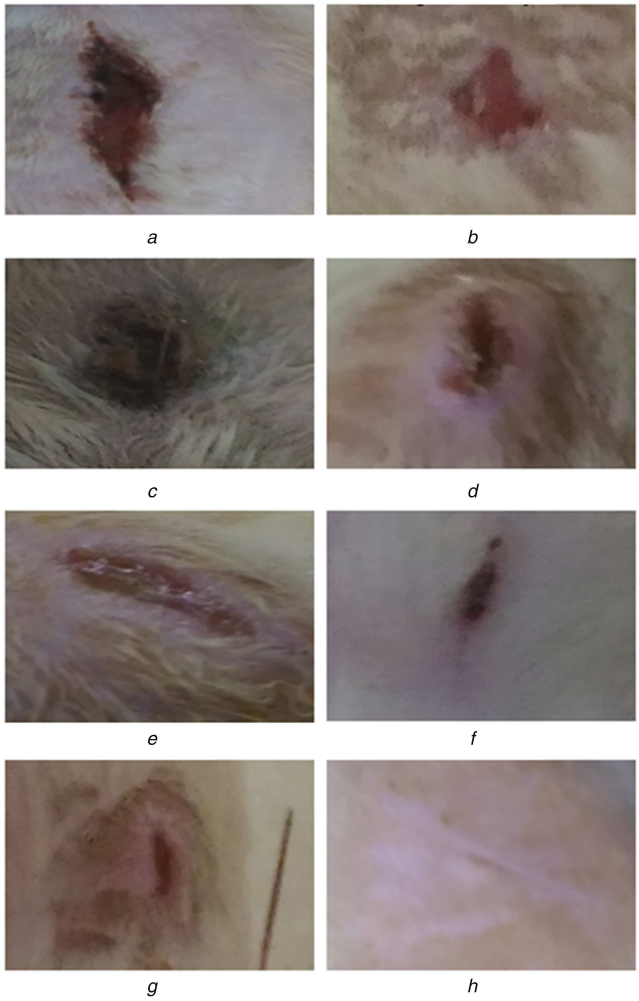

Fig. 4 *Comparison of wound-healing activity of group I (untreated), group II (standard drug), group III (treated with AgNP's) and group IV (treated with Ag–ZnO composite NPs)*

(a) Group I 5th day, ***(b)*** Group I 10th day, ***(c)*** Group II 5th day, ***(d)*** Group II 10th day, ***(e)*** Group III 5th day, ***(f)*** Group III 10th day, ***(g)*** Group IV 5th day, ***(h)*** Group IV 10th day

when compared with the native drug. So, we formulated 1/10th of the drug for its action and carried out the study which showed following results.

The wound-healing activities of group 1 (untreated), group 2 (treated with dermazin as standard drug), group 3 (treated with AgNPs) and group 4 (Ag–ZnO composite NPs) were carried out to determine the rate of wound contraction by excision wound model. The percentage of wound contraction was recorded by observing the change in the wound area of each group of animals. The progressive changes in the wound were monitored day to day and the wound contraction was recorded on 5th and 10th days. However, on the post-wound day (10th), which is after healing for the group IV animals exhibited $95 \pm 3.53\%$ healing. On the other hand, group I animals exhibited $44.58 \pm 3.67\%$ which is due to the self-immunity of animals, whereas the animals treated with AgNPs (group III) animals showed 69.5 ± 2.23 of healing and finally standard treated group (group II) displays 57.5 ± 2.23 of healing which is tabulated in Table 1. On the basis of the photographs shown, it was visualised that the wound size was decreased by the 10th day in group 4 (treated with Ag–ZnO composite NPs).

The potential wound histology studies on the skin sample of various groups were analysed on 0th and 10th days. This showed a completely destroyed layer of epidermis on day 0, and wounds after 10 days which are treated by Ag–ZnO composite NPs showed fibrosis indicating maximum wound-healing efficiency, owing to rapid epithelialisation of skin. Whereas wounds treated with AgNP's showed no fibrosis and might be attributed by poor antibacterial activity of AgNP's when compared with Ag–ZnO composite NPs. Effective re-epithelialisation of skin has not been observed on day 10 in other groups (data not given here). During the course of study, wound-healing activity is found to be expediting with Ag–ZnO composite, whereas the process is found to be delayed in the native gels.

The current research on the development of Ag and Ag–ZnO composite NPs followed by topical gel formulation using Carbapol l934 and its *in vivo* evaluation of wound-healing activity offers a valuable contribution toward the development of new pharmaceutical products with great market potential. The Ag–ZnO composite NPs study on rats demonstrated the superior performance in promoting wound-healing activity when compared with reported literature of various conventional NPs [20–23]. The possible mechanism for this superior wound-healing activity is mainly due to synergistic antimicrobial actions of Ag and Zn followed by inflammation dampening process; this prevents further infections on wound, thus supporting the rapid epithelialisation process by providing suitable environment for wound healing. In addition, Zn due to its character of boosting collagen synthesis and

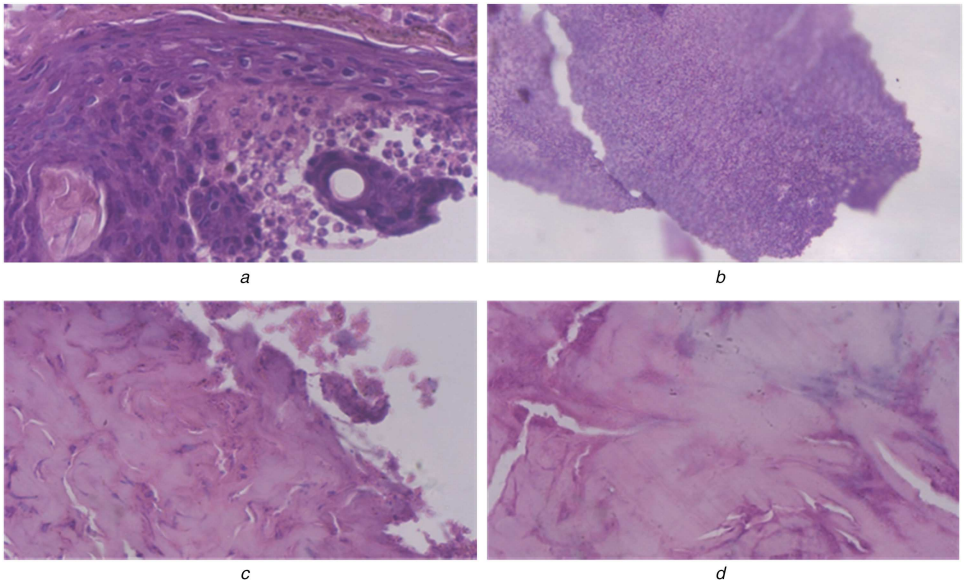

Fig. 5 *Infected skin*

(a), (b) Infected skin with disturbed epidermal layer on the 10th day when treated with AgNPs, ***(c), (d)*** Fibrosis indicating epithelialisation of skin on the 10th day with Ag–ZnO composite NPs

© The Institution of Engineering and Technology 2017

Table 1 Percentage of wound-healing activity against tested sample of groups

Group	Name of the sample	Wound contraction%, mean ± SD	
		5th day	10th day
I	untreated	21.66 ± 3.07	44.58 ± 3.67
II	treated with standard drug	30.8 ± 2.04	57.5 ± 2.23
III*	treated with AgNPs	48.3 ± 2.04	69.5 ± 2.23
IV*	treated with Ag–ZnO composite NPs	61.2 ± 2.62	95 ± 3.53

Values were expressed as mean ± SD for three rats in each group.

Asterisks (*) indicate a statistical significant difference ($P < 0.05$) between the control and the treatments.

rapid re-epithelisation, enhanced the wound-healing process [17, 18]. Zn also has a role in modulating nuclear factor-kappaB-(NFκB) activation and subsequent events during the early inflammatory stage, mRNA levels of the pro-inflammatory cytokines Interleukin 1 beta (IL-1β) and tumor necrosis factor (TNF)-α, target genes of NFκB activation. Owing to their biological roles in the activation of neutrophils, stimulation of fibroblast and keratinocyte growth, synthesis and breakdown of extracellular matrix proteins and regulation of immune responses, it is possible that decreased expression of these cytokines may delay the wound-healing process by impairing tissue regeneration, thus delaying restoration of normal tissue structure and function [24]. The AgNPs known to show efficient antimicrobial properties compared with other Ag compounds due to their large surface area. The extensive surface morphology provides better contact with microorganisms. AgNP interacts with cell membrane and then penetrates inside the cell. Bacterial cell membrane contains proteins, which include sulphur. AgNP interacts with these proteins, as well as with the phosphorus containing compounds such as DNA. Following entry into the bacterial cell, it forms a low molecular weight region at the centre of the bacteria to which the bacteria conglomerate, thus protecting the DNA from the Ag ions. The AgNP interacts with the respiratory chain and cell division finally leading to cell death. This was found while applying AgNP on Gram-positive and Gram-negative bacteria including highly multiresistant strains [25]. More recently, Batarseh's research showed that the bactericidal effect was caused by Ag chelating, which prevents DNA from unwinding. Also they play a role in cytokine modulation and suppress inflammation [26, 27]. In the present paper, the enhanced antibacterial activity of Ag–ZnO NPs might be attributed from the control of Ag ion release similar to mechanism of antibacterial activity [28, 29].

Hence, in this paper the synthesis of Ag–ZnO composite NPs followed by gel formulation is known to be highly efficient, more economical and simple in process for developing the potential topical application with enhanced wound-healing activity. The synergistic antibacterial effect with the combination of Ag and Zn has more potential, when compared with other NPs. Here, we present a possible explanation for the enhancement of the synergistic wound-healing mechanism. This research provides helpful insight into the development of new wound-healing agents. To elucidate the mechanism of this synergistic effect, more elaborate experimental evidence will be needed, and we are currently working toward this end.

4 Conclusion

Synthesis and characterisation of Ag and Ag–ZnO composite NPs and their evaluation toward wound-healing activity in rats were studied. UV–vis spectroscopy of composed Ag and Ag–ZnO composite NPs colloidal solution displayed absorption maxima at 420 nm. SEM, XRD and TEM analyses of Ag–ZnO composite NPs revealed monodispersed hexagonal and quasi-hexagonal morphology with a mean particle size of 20–30 nm. Furthermore, we have tested their wound-healing activity in Wistar Albino rats using AgNPs; Ag–ZnO composite NPs were formulated into a gel by using Carbapol l934 to examine their wound-healing activity. These studies reveal high performance of Ag–ZnO composite toward contraction of wounds when compared with pure AgNPs and standard drug.

5 Acknowledgments

The author thank the University Grants Commission for providing financial assistance and the Andhra university authorities for providing the other necessary laboratory facilities. Authors acknowledge SAIF, IIT Bombay for characterisation facilities.

6 References

[1] Chaloupka, K., Malam, Y., Seifalian, A.M.: 'Nanosilver as a new generation of nanoproduct in biomedical applications', *Trends Biotechnol.*, 2010, **28**, (11), pp. 580–588

[2] Govindarajan, R., Vijayakumar, M., Rao, C.V., *et al.*: 'Healing potential of *Anogeissus latifolia* for dermal wounds in rats', *Acta Pharma.*, 2004, **54**, (4), pp. 331–338

[3] Rozaini, M.Z., Zuki, A.B.Z., Noordin, M., *et al.*: 'The effects of different types of honey on tensile strength evaluation of burn wound tissue healing', *J. Appl. Res. Vet. Med.*, 2004, **2**, pp. 290–296

[4] Baie, S.H.J., Sheikh, K.A.: 'The wound healing properties of *Channa striatuscetrimide* cream-tensile strength measurement', *J. Ethno Pharmacol.*, 2000, **71**, (12), pp. 93–100

[5] Mahendra, R., Alka, Y., Aniket, G.: 'Silver nanoparticles as a new generation of antimicrobials', *Biotechnol. Adv.*, 2009, **27**, (1), pp. 76–83

[6] Kholoud, M.M., Abou, E.N., Alaa, E., *et al.*: 'Synthesis and applications of silver nanoparticles', *Arab. J. Chem.*, 2010, **3**, (3), pp. 135–140

[7] Salata, O.V.: 'Applications of nanoparticles in biology and medicine', *J. Nanobiotechnol.*, 2004, **2**, (3), pp. 1–6

[8] Kumar PPN, V., Pammi, S.V.N., Pratap, K., *et al.*: 'Green synthesis and characterization of silver nanoparticles using *Boerhaavia diffusa* plant extract and their antibacterial activity', *Ind. Crops Prod.*, 2014, **52**, pp. 562–566

[9] Acharyulu, N.P.S., Madhu Kiran, P., Pratap, K., *et al.*: 'Room temperature synthesis and evaluation of antibacterial activity of silver nanoparticles using *Phyllanthus amarus* leaf extract', *J. Bionanosci.*, 2014, **8**, pp. 1–5

[10] Lakshmi, P., Kalyani, K., Hanumanta Rao, N., *et al.*: 'Green synthesis, characterization and antimicrobial activity of silver nanoparticles using methanolic root extracts of *Diospyros sylvatica*', *J. Environ. Sci.*, 2017, **55**, pp. 157–163

[11] Rao N, H., Lakshmidevi, N., Pammi, S.V.N., *et al.*: 'Biosynthesis of silver nanoparticles using methanolic root extracts of *Diospyros paniculata* and their antimicrobial activities', *Mater. Sci. Eng. C*, 2016, **62**, pp. 553–557

[12] Benjamin, L.O., Francesco, S.: 'Antibacterial activity of silver nanoparticles: a surface science insight', *Nano Today*, 2015, **10**, pp. 339–354

[13] Fidel, M.G., Emily, P.T., Judith, M.S., *et al.*: 'Antibacterial activity, inflammatory response, coagulation and cytotoxicity effects of silver nanoparticles', *Nanomed., Nanotechnol., Biol. Med.*, 2012, **8**, pp. 328–336

[14] Asharani, P.V., Mun, G.L.K., Hande, M.P., *et al.*: 'Cytotoxicity and genotoxicity of silver nanoparticles in human cells', *ACS Nano*, 2009, **3**, (2), pp. 279–290

[15] Agnihotri, S., Bajaj, G., Mukherji, S.: 'Arginine-assisted immobilization of silver nanoparticles on ZnO nanorods: an enhanced and reusable antibacterial substrate without human cell cytotoxicity', *Nanoscale*, 2015, **7**, (16), pp. 7415–7429

[16] Patil, S., Patil, R., Kale, S., *et al.*: 'Nanostructured microspheres of silver @ zinc oxide: an excellent impeder of bacterial growth and biofilm', *J. Nanoparticle Res.*, 2014, **16**, (11), pp. 1–11

[17] Sudheesh Kumar, P., Lakshmanan, V.K., Anilkumar, T., *et al.*: 'Flexible and microporous chitosan hydrogel/nano ZnO composite bandages for wound dressing: in vitro and in vivo evaluation', *ACS Appl. Mater. Interfaces*, 2012, **4**, (5), pp. 2618–2629

[18] Lansdown, A.B., Mirastschijski, U., Stubbs, N., *et al.*: 'Zinc in wound healing: theoretical, experimental, and clinical aspects', *Wound Repair Regen.*, 2007, **15**, (1), pp. 2–16

[19] Bhaskar, D., Imran Khan, M.D., Jayabalan, R., *et al.*: 'Understanding the antifungal mechanism of Ag@ZnO core-shell nanocomposites against *Candida krusei*', *Sci. Rep.*, 2016, **6**, (1–12), p. 36403

[20] Bhuvaneswari, T., Thiyagarajan, M., Geetha, N., *et al.*: 'Bioactive compound loaded stable silver nanoparticle synthesis from microwave irradiated aqueous extracellular leaf extracts of *Naringi crenulata* and its wound healing activity in experimental rat model', *Acta Trop.*, 2014, **135**, pp. 55–61

[21] Anu, G., Vinay, K., Anu, G., *et al.*: 'Chitosan-based copper nanocomposite accelerates healing in excision wound model in rats', *Eur. J. Pharmacol.*, 2014, **731**, pp. 8–19

[22] Sivaranjani, V., Philominathan, P.: 'Synthesis of titanium dioxide nanoparticles using *Moringa oleifera* leaves and evaluation of wound healing activity', *Wound Med.*, 2016, **12**, pp. 1–5

[23] Abhishek, K., Amit, K.M., Mahesh, K., *et al.*: 'An investigation of in vivo wound healing activity of biologically synthesized silver nanoparticles', *J. Nanoparticle Res.*, 2014, **16**, (1–10), p. 2605

[24] Yunsook, L., Levy, M., Tammy, M.B.: 'Dietary zinc alters early inflammatory responses during cutaneous wound healing in weanling CD-1', *Mice J. Nutr.*, 2004, **134**, pp. 811–816

© The Institution of Engineering and Technology 2017

[25] Marek, K., Tatsiana, D., Aleksandra, M., *et al.*: 'Certain aspects of silver and silver nanoparticles in wound care: a mini review', *J. Nanomater.*, 2016, **47**, pp. 1–10
[26] Lang, D., Xindi, S., Xiaoliang, Z., *et al.*: *Carbohydr. Polym.*, 2017, **157**, pp. 1538–1547
[27] Subhamoy, D., Aaron, B.B.: 'Biomaterials and nanotherapeutics for enhancing skin wound healing front', *Bioeng. Biotechnol.*, 2016, **4**, (1–20), p. 82
[28] Elango, M., Deepa, M., Subramanian, R., *et al.*: 'Synthesis, characterization of polyindole/Ag–ZnO nanocomposites and its antibacterial activity', *J. Alloys Compd.*, 2017, **696**, pp. 391–401
[29] Zhong, L., Jingting, G., Qingfeng, H., *et al.*: 'Enhanced antibacterial and wound healing activities of microporous chitosan–Ag/ZnO composite dressing', *Carbohydr. Polym.*, 2017, **156**, pp. 460–469

© The Institution of Engineering and Technology 2017